

¹ Marine Science Program, School of Environmental and Natural Resource Sciences,
Faculty of Science and Technology, National University of Malaysia, Bangi, Selangor, Malaysia
² Department of Oceanography, University of Cape Town, Rondebosch, South Africa
³ Malaysian Meteorological Department, Petaling Jaya, Selangor, Malaysia

Simulation of tropical cyclone Vamei (2001) using the PSU/NCAR MM5 model

L. Juneng¹, F. T. Tangang¹, C. J. C. Reason², S. Moten³, and W. A. W. Hassan³

With 16 Figures

Received June 2, 2006; accepted January 6, 2007
Published online: March 14, 2007 © Springer-Verlag 2007

Summary

In this study, a rare tropical cyclone Vamei was simulated using the non-hydrostatic version 3.6 of the Penn State University (PSU) – National Center for Atmospheric Research (NCAR) mesoscale model MM5. This unusual cyclone was generated on 26 December 2001 in an area close to the equator in the southern part of the South China Sea. The model was integrated for 80 h from 0000 UTC 26 December 2001 to 1800 UTC 29 December 2001. To examine the model performance, several important simulated fields including sea-level pressure, surface wind speed and precipitation were compared to observations. The model simulated track of the cyclone was also compared to the best track provided by the Joint Typhoon Warning Center (JTWC). Overall, the model performed reasonably well, particularly in simulating the cyclone track and precipitation amount and spatial distribution. The analysis of the model output indicated the important role of the latent heat flux in the genesis and intensification of tropical cyclone Vamei.

1. Introduction

The occurrence of tropical cyclones equatorward of 5° latitude is considered rare. This is due to the reduction of the Coriolis effect that is needed for significant rotational motion (e.g., Anthes, 1982; Holliday and Thompson, 1986). However,

on 0600 UTC 27 December 2001, a very unusual tropical cyclone (named Vamei by the Japan Meteorological Agency, JMA) was generated near 60 km east of the tip of the southern Malay Peninsula with its centre located at about 1.5° N. Interestingly, this was the first ever-recorded tropical cyclone formation at such a low latitude. Since 1886, two other near-equatorial typhoons have been generated within 5° of the equator. In March 1956, typhoon Sarah formed at 4° N latitude (Fortner, 1958). During 13–18 October 1970, typhoon Kate was generated at about 5° N in the western North Pacific region (Holliday and Thompson, 1986). Due to its near-equatorial location, the southern part of South China Sea (SCS) is considered to be cyclone-free region. Hence, the region encompassing the Malay Peninsula and Borneo has never experienced the disastrous impact of a typhoon prior to the occurrence of Vamei. It was reported in the local media that Vamei caused severe flooding and mudslides in the southern Malay Peninsula's Johor and Pahang states with more than 17,000 people evacuated and five reported deaths.

Due to the unfavorable conditions for typhoon formation in the region, it is of interest to inves-

tigate the cyclogenesis of typhoon Vamei. To date, there has been only a single investigation into Vamei formation (Chang et al, 2003). Chang et al (2003) hypothesized that this rare tropical storm was formed when a weak vortex located over western Borneo drifted into a narrow region of the southern SCS and interacted with a northeast monsoon cold surge that intruded into the region. The Borneo vortex is a persistent quasi-stationary low-level circulation feature in western Borneo during boreal winter (Johnson and Houze, 1987; Chang et al, 2003). Cold surges from East Asia in boreal winter often act to enhance the Borneo vortex and to shift the centre of the vortex to the western coast of Borneo (Chang et al, 2005). According to Chang et al (2003), the formation of Vamei was initiated when a strong northeasterly winter monsoonal surge slightly deflected to the northwest of the vortex and consequently, the cross-equatorial flow was wrapped around the vortex resulting in a rapid counterclockwise rotation. Vamei cyclogenesis appears to be consistent with the theory of equatorial cyclogenesis proposed by Lim and Chang (1981). According to Lim and Chang (1981), equatorial cyclogenesis is dynamically possible and can be demonstrated using equatorial wave theory. According to this theory, geostrophic adjustment and vorticity conservation following a cross-equatorial surge spins up a counterclockwise ro-

tation to the east of the surge axis. At the time of Vamei, the Borneo vortex was located east of the surge axis. Chang et al (2003) concluded that typhoon Vamei was indeed a rare phenomenon with an estimated probability of occurrence of once every 100–400 years.

In this paper, we present a numerical simulation of Vamei using the Pennsylvania State University (PSU)/National Center for Atmospheric Research (NCAR) Fifth Generation Mesoscale Model MM5 Version 3.6 (PSU/NCAR MM5 v3.6). This model has been shown to have simulated various tropical cyclones with reasonable accuracy (e.g., Liu et al, 1997; Farfán and Zehnder, 2001; Power and Davis, 2002; Mohanty et al, 2004). However, it has never been used to simulate a near-equatorial cyclone. It is of interest to see whether MM5 is capable of simulating the tropical cyclone Vamei, particularly when its circulation extends to both sides of the equator.

This paper is organized as follows. The next section describes the data sets used for documenting the evolution of Vamei and the numerical simulation. Section 3 provides a brief overview of typhoon Vamei. In Sect. 4, we provide a detailed description of the model configuration and setup. Section 5 provides results, validation, and further diagnosis of the storm based on the simulation output. A summary and conclusion is presented in Sect. 6.

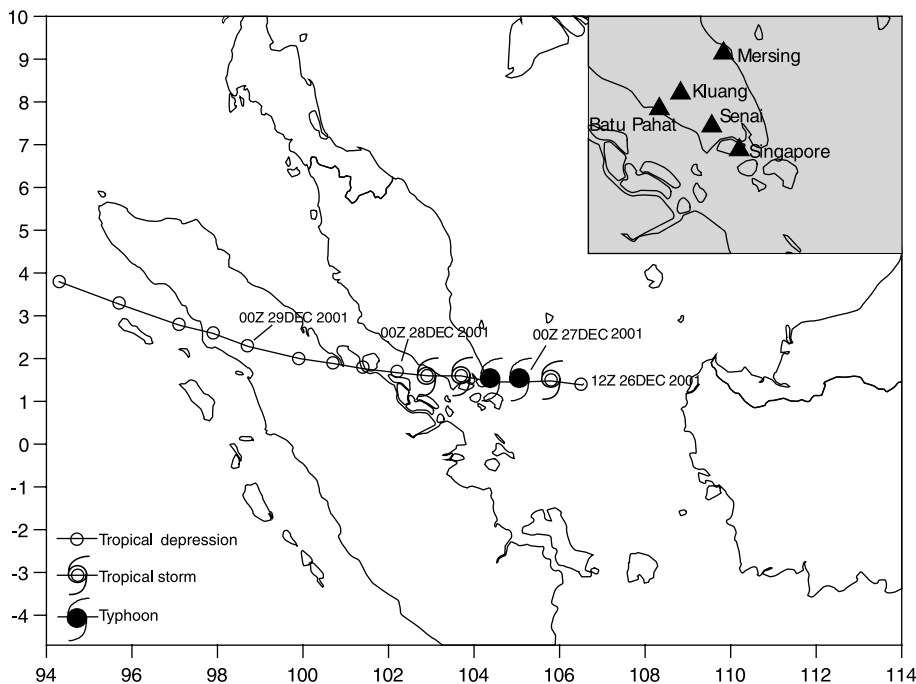


Fig. 1. The propagating track of Vamei and the centre of the vortex updated 6-hourly as archived in JTWCs best track database. The upper-right box shows the location of the local surface observational stations used in the study

2. Data

We use several data sets to document the evolution of Vamei and to define the inputs to the PSU/NCAR MM5 model. These include Special Sensor Microwave Imager (SSM/I) imagery and Tropical Rainfall Measuring Mission (TRMM) three hourly rainrate. We also derived the evolution and development of the storm based on the Joint Typhoon Warning Center (JTWC) best track database for the period 1200 UTC 26 December to 00 UTC 30 December. These include the maximum sustained surface wind and storm central pressure available at 6-hour intervals. Various local surface station data were obtained from the Malaysian Meteorological Department (MMD). These include hourly recorded surface pressure,

surface wind speed and hourly precipitation at four local surface observational stations (Senai, Kluang, Batu Pahat, Mersing) located in the southern Malay Peninsula (see Fig. 1). For the surface wind speed data, an additional record from Singapore is also provided. The initial and lateral boundary conditions needed by MM5 were obtained from the Naval Operational Global Atmospheric Prediction System (NOGAPS) operational product of the US Global Ocean Data Assimilation Experiment (USGODAE) at the Fleet Numerical Meteorology and Oceanography Center (FNMOC). The SST used in the model is the weekly Reynold SST (Reynolds and Smith, 1994) data provided by the NOAA-CIRES Climate Diagnostics Center, Boulder, Colorado,

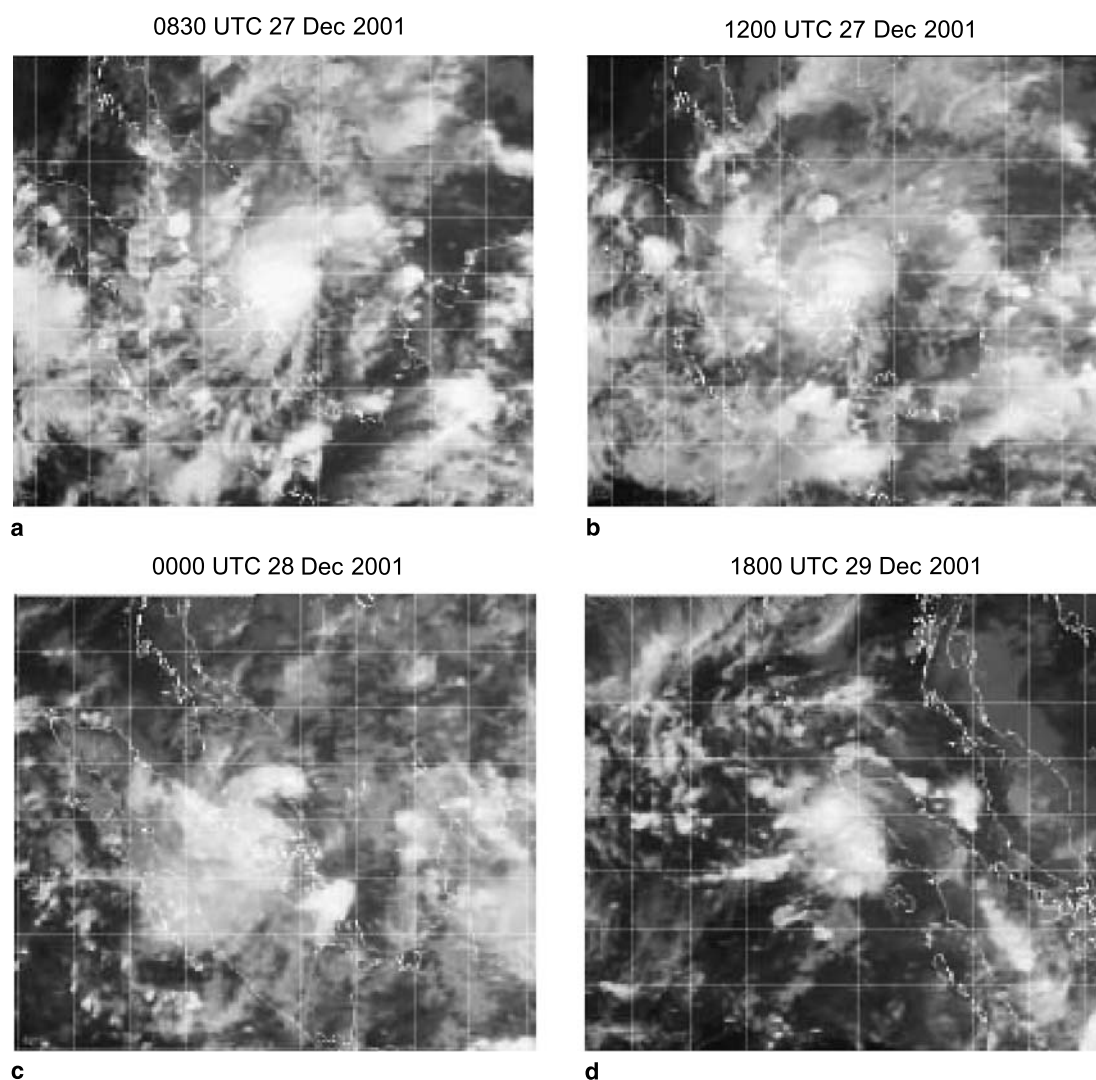


Fig. 2. SSM/I imagery of IR temperature taken at (a) 0830 UTC 27 December, (b) 1200 UTC 27 December, (c) 00 UTC 28 December, and (d) 1800 UTC 29 December

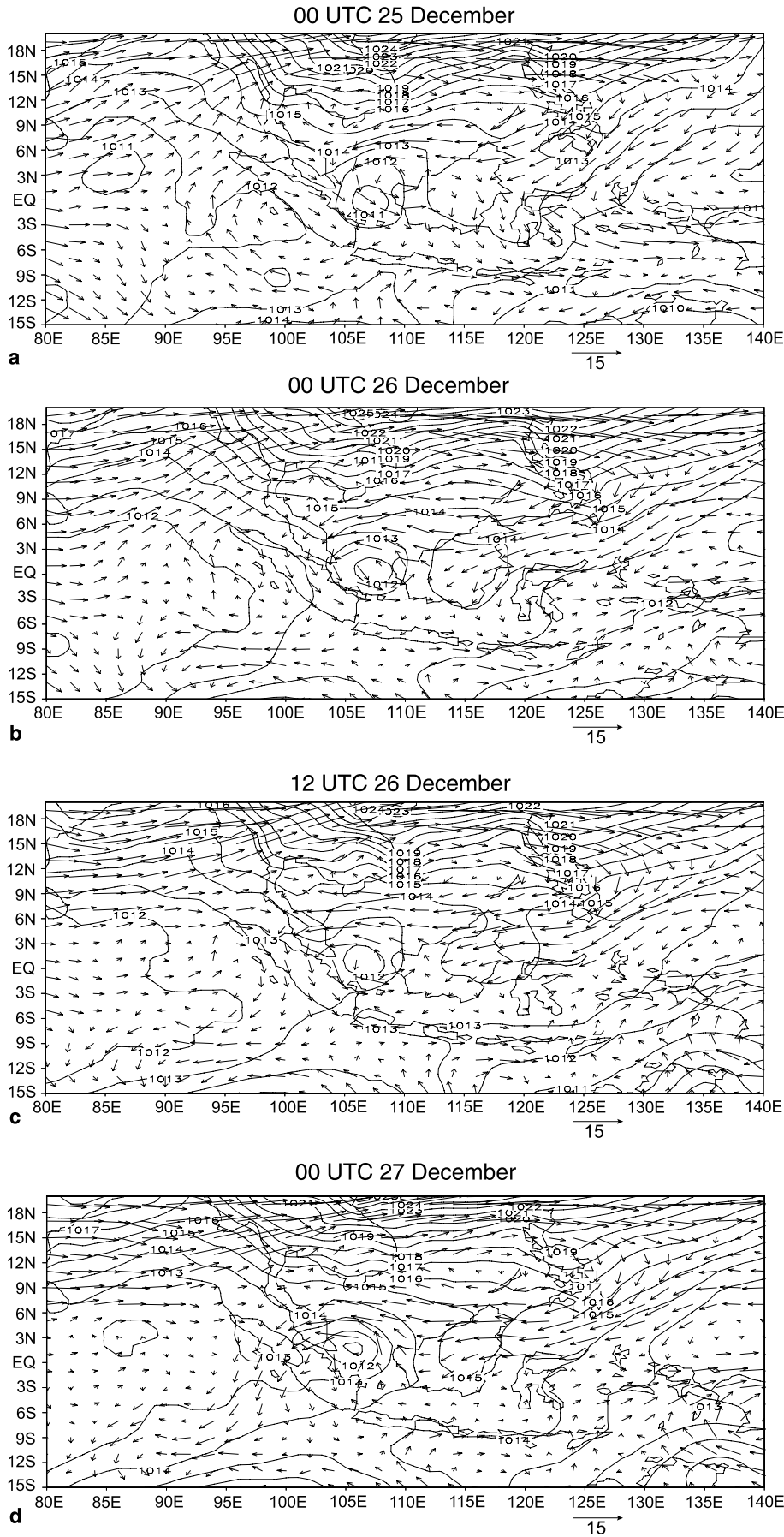


Fig. 3. Mean sea-level pressure (contour) and 500 hPa horizontal winds from NOGAPS at (a) 00 UTC 25 December, (b) 00 UTC 26 December, (c) 12 UTC 26 December 2001, and (d) 00 UTC 27 December 2001. A scale vector (m s^{-1}) is shown at the bottom of each panel

USA, from their Web site at <http://www.cdc.noaa.gov/>.

3. Overview of tropical cyclone Vamei

Figure 1 shows the track followed by the tropical cyclone Vamei based on the best-track positions provided by the JTWC. The track indicates that the early development of Vamei took place in the narrow region of the southern part of the SCS. At 1200 UTC 26 December 2001, the system was classified as a tropical depression with its centre located at about 1.5°N and 106.5°E . The system intensified as it moved westward toward the southern tip of the Malay Peninsula where the system attained the strength of a typhoon before it made landfall. Immediately after landfall, the system weakened and was reclassified as a tropical storm. The system further weakened as it continued its westward movement across the Strait of Malacca and was downgraded to a tropical depression when it reached Sumatra. The westward movement of the system continued across

Sumatra to the eastern Indian Ocean where it dissipated.

The development of tropical cyclone Vamei is associated with the southward intrusion of a winter monsoon northeasterly surge over the SCS and the Borneo vortex that drifted into the southern part of SCS (Chang et al, 2003). They reported that early on 19 December 2001, a cold surge penetrated rapidly over the SCS while the Borneo vortex was established at the northwest coast of Boreno at approximately 3°N . On 21 December 2001, the vortex drifted off the coast to the narrow part of the southern SCS i.e., the region between western Borneo and the eastern Malay Peninsula and persisted in the area for several days. The strong northeasterly surge was slightly deflected to the northwest of the vortex causing the cross-equatorial flow to wrap around the vortex resulting in a spinning up of a rapid counter-clockwise circulation (Chang et al, 2003).

Based on the JTWC Annual Tropical Cyclone 2001 Report, at 0600 UTC 25 December, the

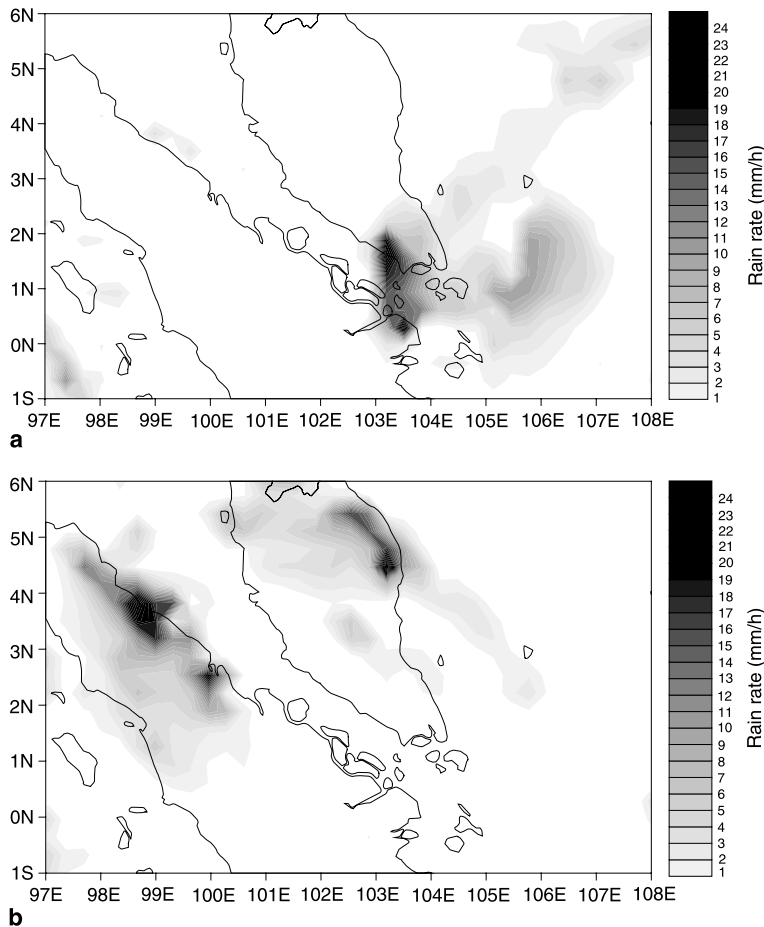


Fig. 4. Surface rainrate (unit in mm/hour) at (a) 0000 UTC–0300 UTC 27 December 2001, and (b) 1200 UTC–1500 UTC 27 December 2001 from TRMM 3 hourly product

centre was located approximately 370 km north-east of Singapore and moving toward the southern tip of the Malay Peninsula. At 0600 UTC 26 December, the system was classified as tropical depression and was located about 241 km northeast of Singapore. By late on 26 December, the depression began to strengthen rapidly and it was upgraded to tropical storm intensity at 1800 UTC 26 December with a reported maximum surface wind of approximately 18 m s^{-1} .

Six hours later at 0000 UTC 27 December, based on the naval ship observations indicating sustained wind of 33 m s^{-1} , Vamei was upgraded to a typhoon by JTWC with its centre located approximately 139 km east of Singapore. On the other hand, JMA reported that the system remained at tropical storm intensity as indicated in the 2001 Annual Report of the Regional Specialized Meteorological Center (RSMC), Tokyo Typhoon Center.

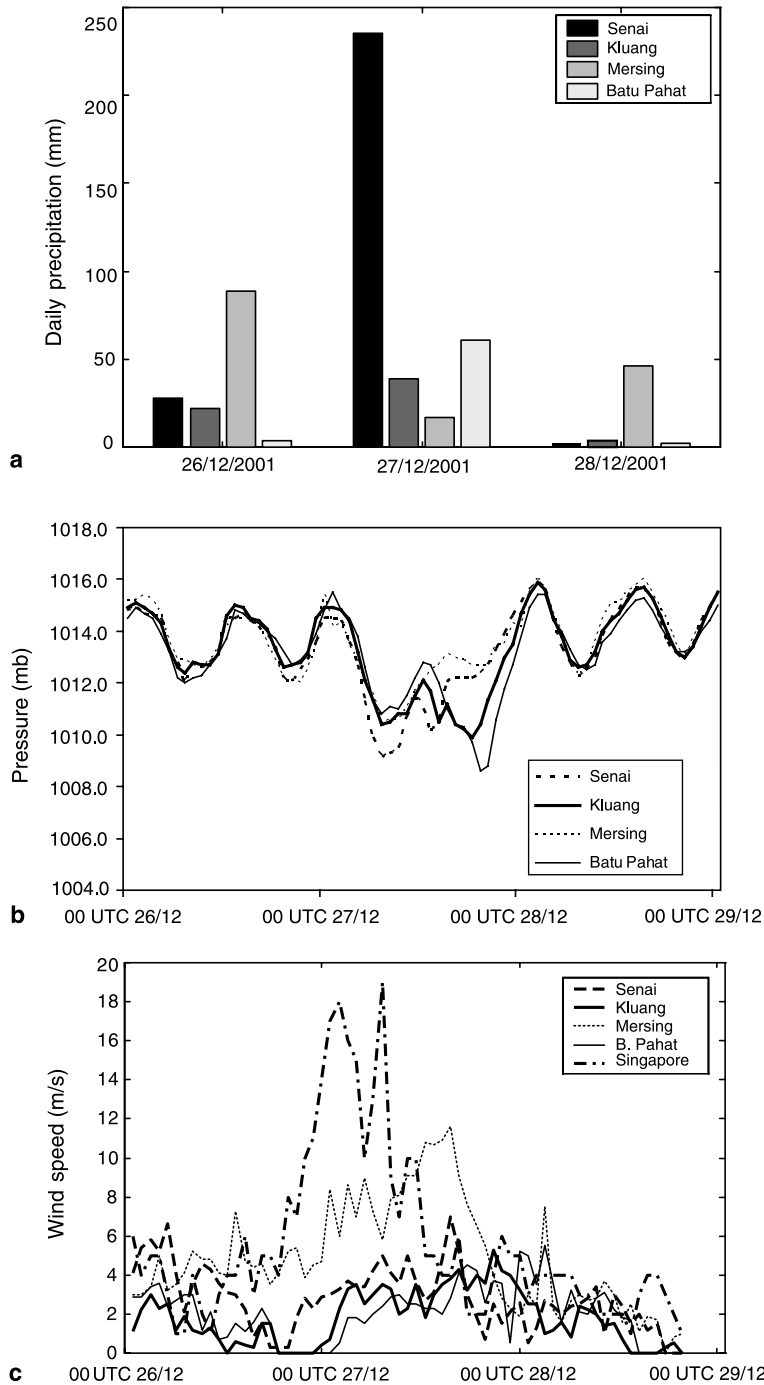


Fig. 5a. Daily rainfall recorded at Senai, Kluang, Mersing and Batu Pahat. The accumulated values are computed from 00 UTC to 00 UTC the next day. **(b)** Surface pressure (in mb) recorded at all four stations as in **(a)**. **(c)** The recorded surface wind speed (unit in meter per second) with addition record from Singapore station

Typhoon Vamei propagated rapidly westward and made landfall on the southeastern tip of the Malay Peninsula at about 0830 UTC 27 December (JTWC). The infrared image taken at 0830 UTC 27 December clearly indicates an intense convective system with a centre located at the tip of the Peninsula (Fig. 2a). At 1200 UTC, the system was located over the southern part of the Peninsula about 37 km north of Singapore (Fig. 2b). The storm weakened rapidly after it made landfall and tracked slightly northwestward (Fig. 1). By 0000 UTC 28 December, Vamei was over Sumatra (Fig. 2c) when both the JTWC and JMA downgraded the system to a tropical depression. By 1800 UTC 29 December, the remnants of Vamei was already west of northern Sumatra (Fig. 2d) where it continued its westward propagation until 1800 UTC 31 December when JTWC gave their final warning on the system.

The westward track followed by Vamei may be explained by the structure of the synoptic-scale monsoonal flow at middle levels. Figure 3 indicates the sequence of NOGAPS mean sea-level pressure and the 500 hPa horizontal wind field taken at 00 UTC 25 December, 0000 UTC and 1200 UTC 26 December and 00 UTC 27 December. At 00 UTC 25 December, before the strengthening of the system, the background flow is characterised by a northeasterly monsoonal flow east of the southern Philippines which turned into a northwesterly flow after crossing the equator just east of Borneo (Fig. 3a). Also noted is

the existence of an anticyclone circulation centered to the west of Sumatra. The westerlies over Sumatra and the Malay Peninsula on December 25 interacted with the low pressure disturbance in the SCS (Vamei). This circulation pattern was also a persistent feature a few days prior to 25 December 2001 (not shown) and hence may have enabled the system to linger in the southern part of SCS long enough for cyclogenesis to occur. Chang et al (2003) suggested that the fact that the system remained in the southern SCS is an important factor for the cyclogenesis of Vamei. After 00 UTC 26 December, the monsoonal flow east of the Philippines strengthened and the northwesterly flow south of the equator weakened rapidly (Fig. 3b–d). By 12 UTC 26 December, relatively strong easterlies existed from the southern Philippines, across Borneo and into the SCS and therefore acting as a westward steering current facilitating propagation of Vamei across the Malay Peninsula and Sumatra. Following the strengthening of the easterly steering flow, also noted is the weakening of the anticyclone west of Sumatra (Fig. 3b–d).

The system brought heavy rainfall as it crossed the southern tip of the Malay Peninsula into the Strait of Malacca and Sumatra. Several hours before it made landfall, the southern tip of the Malay Peninsula received substantial amount of rain as indicated by the TRMM 3 hourly rainrate of 0000 UTC–0300 UTC 27 December 2001 with the heaviest rainfall occurring at the eastern

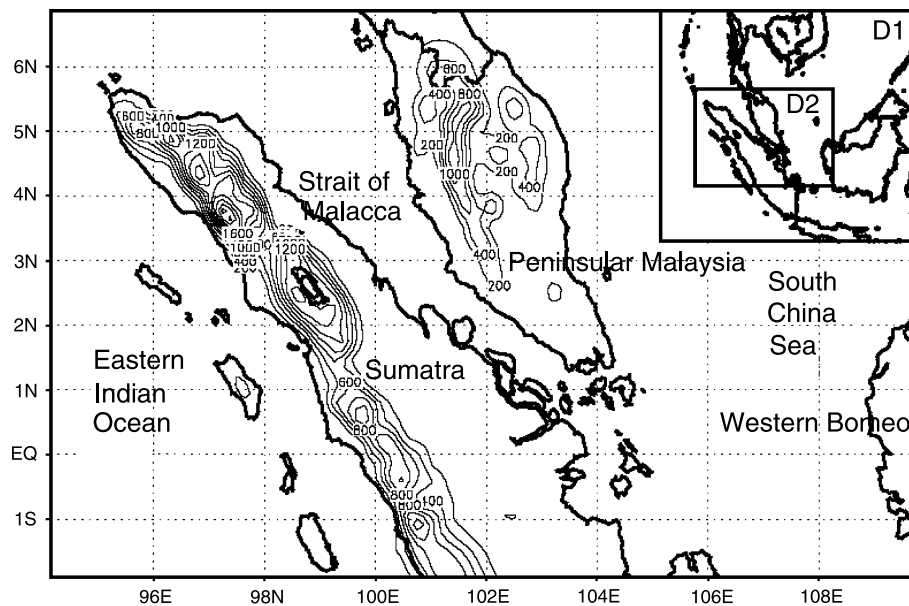


Fig. 6. The upper-right box depicts both the defined coarse (D1) and fine (D2) domains used in the numerical simulation. The regular box shows the high resolution D2 together with the terrain elevation height (m)

side (Fig. 4a). During 1200 UTC–1500 UTC 28 December when the system was over northern Sumatra, heavy precipitation occurred both over the northeastern part of Sumatra and Malay Peninsula (Fig. 4b).

Several local observing stations also recorded heavy rainfall during the passage of the sys-

tem. During 26 December 2001, when the system was still developing over the SCS, Mersing station (see Fig. 1) received heavy precipitation with amounts near 100 mm (Fig. 5a). As the system moved over land on 27 December, Senai station recorded the heaviest precipitation of more than 200 mm. However, as the system moved

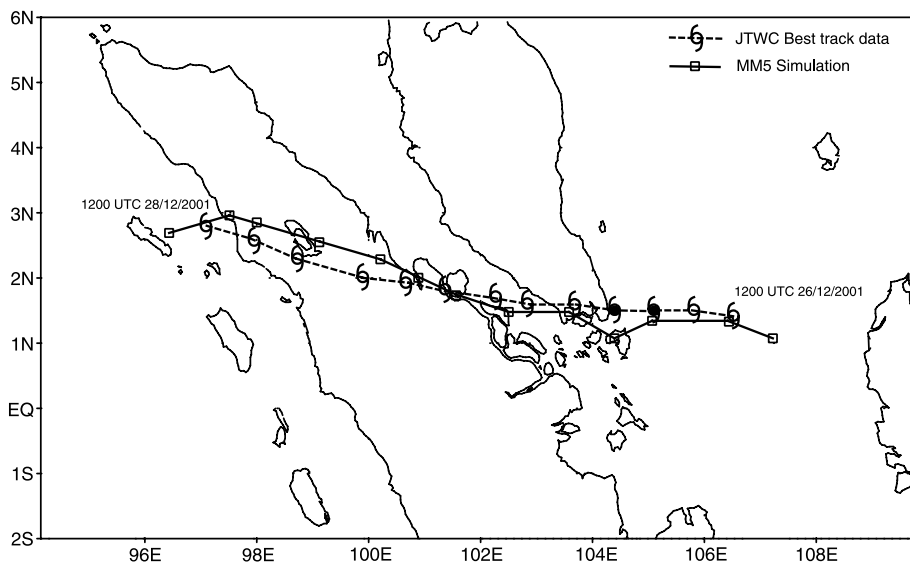


Fig. 7. The simulated (squares) storm track updated at 6-hourly. The simulated storm position is computed based on 850 hPa vorticity maxima. JTWC’s best track (dot) is also provided for comparison purpose

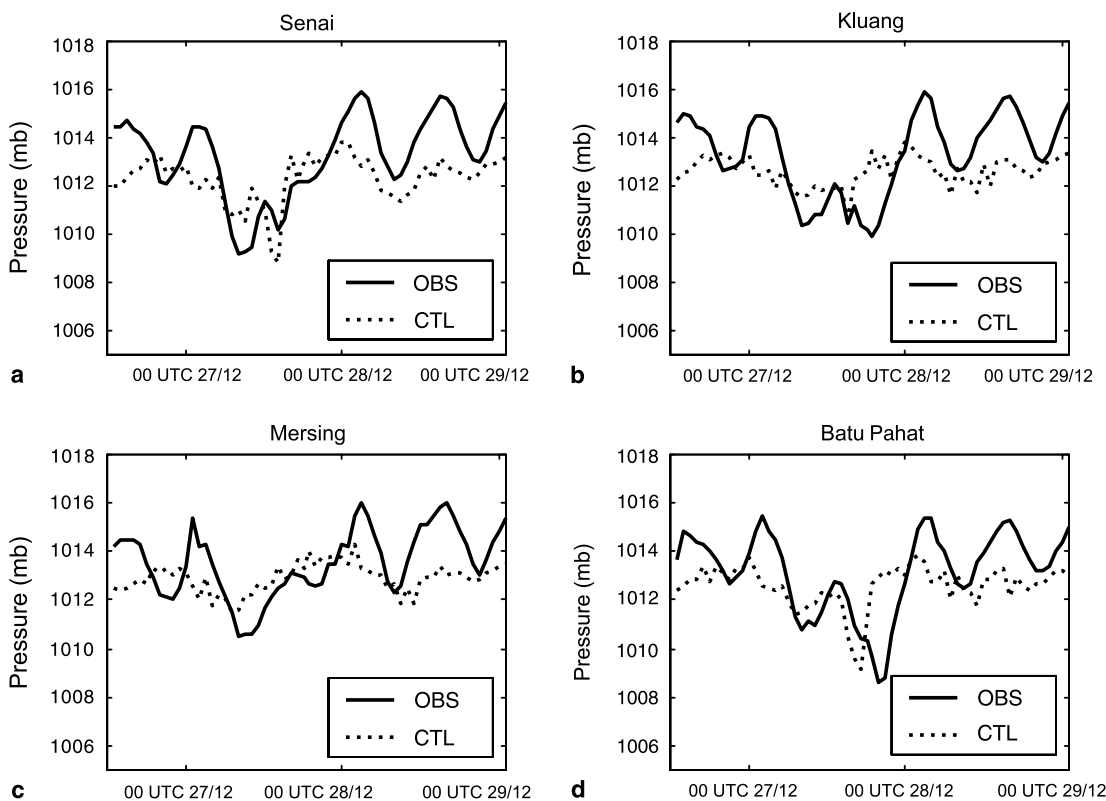


Fig. 8. Simulated (dotted) and the recorded (solid) surface pressure (mb) at (a) Senai, (b) Kluang, (c) Mersing, and (d) Batu Pahat

across the Strait of Malacca and over Sumatra Island on 28 December, all stations except Mersing recorded minimal precipitation. The lowering of surface pressure as the system crossed the southern tip of the Malay Peninsula during 27 to 28 December was recorded at all stations (Fig. 5b). However, the surface wind speeds at all three stations, i.e., Senai, Kluang and Batu Pahat, were less than 6 m s^{-1} during the period. Mersing and Singapore stations recorded a rapid strengthening of the wind speed up to 12 m s^{-1} and over 17 m s^{-1} , respectively, during the period (Fig. 5c).

4. Model configuration

The MM5 version 3–6 model is used for the present study. MM5 is a limited area, non-hydrostatic, terrain-following sigma-coordinate model. A total of 31 σ -layers were used in the vertical up to 100 hPa. In this study, a two-way interactive nested grid capability (Zhang et al, 1986) was implemented. Two horizontal grids were used with the coarse domain (D1) at 45 km resolution and an inner domain (D2) at 15 km grid resolution (Fig. 6). The terrain elevation and land-use/vegetation used in the simulation were obtained from the US Geophysical Survey (USGS) 25-

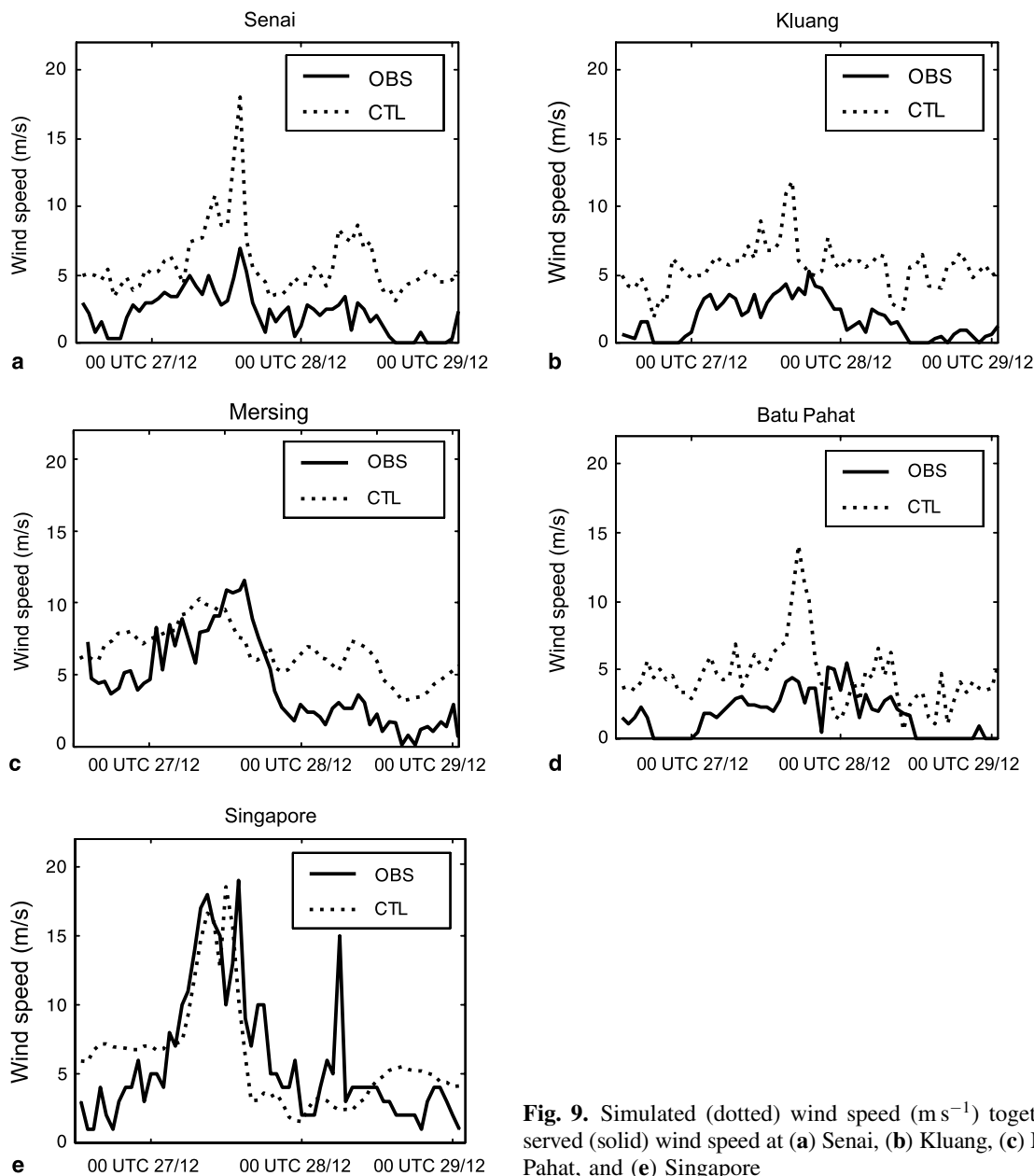


Fig. 9. Simulated (dotted) wind speed (m s^{-1}) together with the observed (solid) wind speed at (a) Senai, (b) Kluang, (c) Mersing, (d) Batu Pahat, and (e) Singapore

category global dataset. Planetary boundary layer processes were parameterized with the high-resolution Blackadar scheme (Zhang and Anthes, 1982) while the Kain-Fritsch scheme (Kain and Fritsch, 1993) was used for convection. The explicit moisture scheme based on Schultz (1995) that contains ice and graupel/hail processes was also implemented. The NCAR/CCM2 radiation scheme was used. Identical parameterizations were used in both domains for consistency. The initial and lateral boundary conditions, updated at 12 hours interval, were derived from the operational product of NOGAPS. The Reynold SST obtained from the Climate Diagnostic Center (CDC2) was held constant throughout the simulation period. The duration of the model run was from 00 UTC 26 December 2001 until 1800 UTC 29 December 2001. The model outputs were validated with local datasets (sea-level pressure (SLP), rainfall, surface wind) obtained from the MMD, TRMM rainrates and JTWC's best track.

5. Analysis of model run

5.1 Validation of the simulation

Figure 7 displays the simulated storm track (in D2) plotted together with the observed position of the storm centre at 6 hours interval from the JTWCs best track database. The simulated storm position was computed by tracking the location of the 850 hPa maximum vorticity. The simulated storm position was generally in good agreement with the JTWCs best track. However, despite the good agreement, there are several discrepancies between the two tracks. The position of the simulated storm at 12 UTC 26 December is located slightly east of the observed location (Fig. 7). Before the simulated storm made landfall, it moved southwestward and later turned northwestward resulting in it landing near the southwestern tip of the Malay Peninsula, i.e., slightly west of the actual landfall position. Also, after the storm reached Sumatra, it diverged slightly northwestward from the observed track.

We compared the observed values of various surface parameters to the simulated values at the closest model grid points to the observation stations. The deepening of the surface pressure at various stations during the passage of Vamei appears to be reasonably well simulated by the

model although the deepening occurred slightly early at Mersing and Batu Pahat stations (Fig. 8). The model also reasonably estimated the fluctuation of wind surface speeds at all stations except the magnitudes were overestimated at three of the stations (Senai, Kluang, and Batu Pahat) (Fig. 9). However, at Singapore, both the magnitude and fluctuation of the surface wind speed were well simulated by the model (Fig. 9e).

Figure 10a and b indicates the simulated 3-hours accumulated precipitation for the two periods of 0000 UTC 27/12–0300 UTC 27/12 and 1200 UTC 28/12–1500 UTC 28/12, respectively. Comparing these figures with the corresponding observed TRMM 3-hourly rainrates of the same periods (Fig. 4), it appears that the distribution of the simulated precipitation was shifted slightly eastward. During the period of 0000 UTC 27/12–0300 UTC 27/12, the heaviest simulated precipitation occurred just east of the

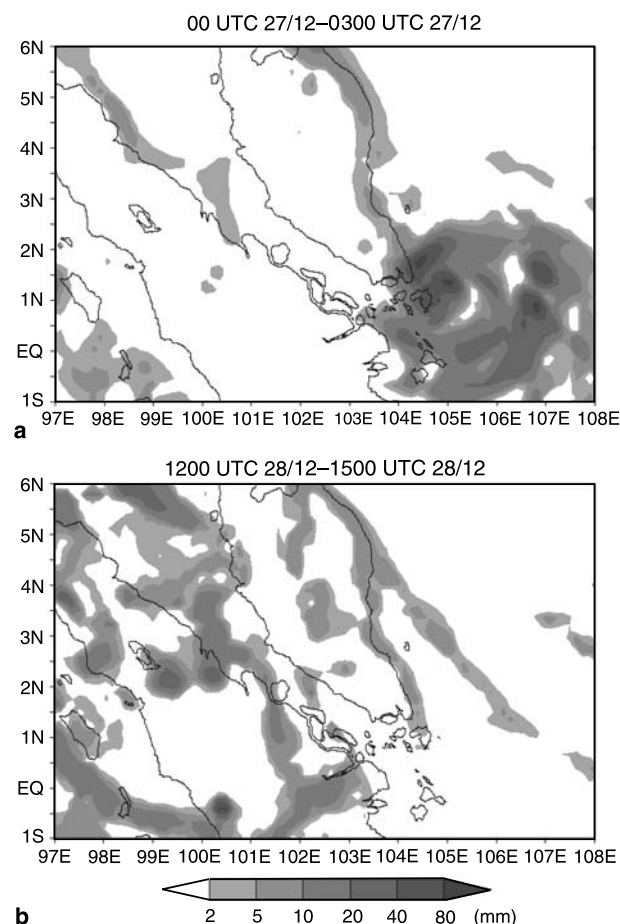


Fig. 10. Simulated 3-hourly accumulated rainfall valid at (a) 00 UTC 27/12–0300 UTC 27/12, and (b) 1200 UTC 28/12–1500 UTC 28/12. The unit is in mm

tip of the Malay Peninsula. The observed TRMM rainrates for the period show that the heaviest rainfall occurred at the western side. This discrepancy could be attributed to the southwestward displacement of the simulated storm 12 hours prior to landing (see Fig. 7). Also during the period of 1200 UTC 28/12–1500 UTC 28/12, the heaviest rainfall occurred over the Strait of Malacca and not over the northeastern region of Sumatra as indicated by the observed TRMM rain rates in Fig. 4b. This discrepancy could be due to the northward displacement of the simulated storm after it reached Sumatra landmass (see Fig. 7). The heavy rainfall over the northeastern coastal region of the Malay Peninsula is well simulated in the model.

Figure 11 depicts the simulated versus observed accumulated rainfall at various stations during the period from 1200 UTC 26/12 to 0000 UTC 29/12. The model reasonably simulated the accumulated rainfall at the stations of Mersing and Batu Pahat (and to lesser extent at Kluang) with total 54-hour accumulated rainfall values fairly close to that observed. Note that the sudden increase in precipitation at Batu Pahat at around 12 UTC 27/12 was captured in the simulation. However, the simulation considerably underestimated the accumulated rainfall at Senai (Fig. 10a). This issue was investigated further because this region received more than 200 mm of rainfall during the passage of Vamei on 27 December 2001 as indicated by the recorded val-

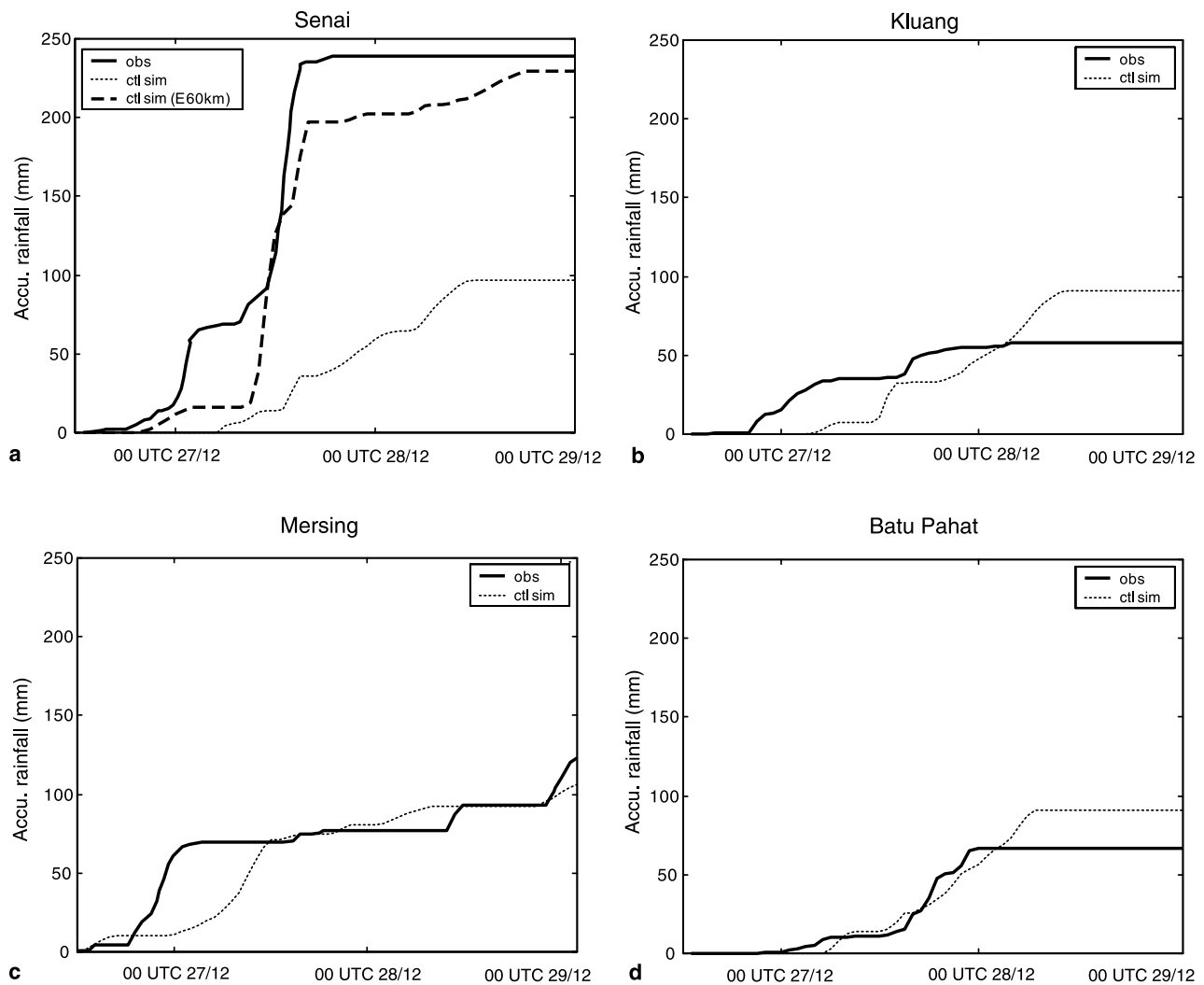


Fig. 11. Observed (solid) and simulated (dotted) accumulated rainfall (mm) since 12 UTC 26 December 2001 at (a) Senai, (b) Kluang, (c) Mersing, and (d) Batu Pahat. The dark dotted line in (a) is the simulated accumulated precipitation at grid 104.2° E longitude and 1.6° N. Please refer text for further details

ues at Senai (Fig. 5a). The simulated accumulated rainfall was less than half of that observed whereas at the other stations, the model simulated accumulated totals were much closer to the observations. Examination of the model output shows that the simulation actually reproduced the rainfall amount correctly but with the centre of rainfall maxima shifted ~ 60 km to the east of Senai toward the east coast of southern Malay Peninsula. A comparison between Senai (103.6° E; 1.6° N) recorded accumulated rainfall with the rainfall simulated at 104.2° E longitude and 1.6° N latitude grid depicts a similar curve with both registering more than 200 mm at the end

of the comparison period. The sudden increase in rainfall at around 0800 UTC 27 December is also seen in both the observation and simulation. These results suggest that the simulation reproduced most of the main rainfall characteristics associated with tropical cyclone Vamei reasonably well despite a slight eastward shift of the centre of rainfall maxima. As discussed earlier, this shift is possibly associated with the southward deviation in the model before landfall which occurred a little west of its observed location (see Fig. 7).

Figure 12 shows the comparison of the central pressure and maximum surface wind between

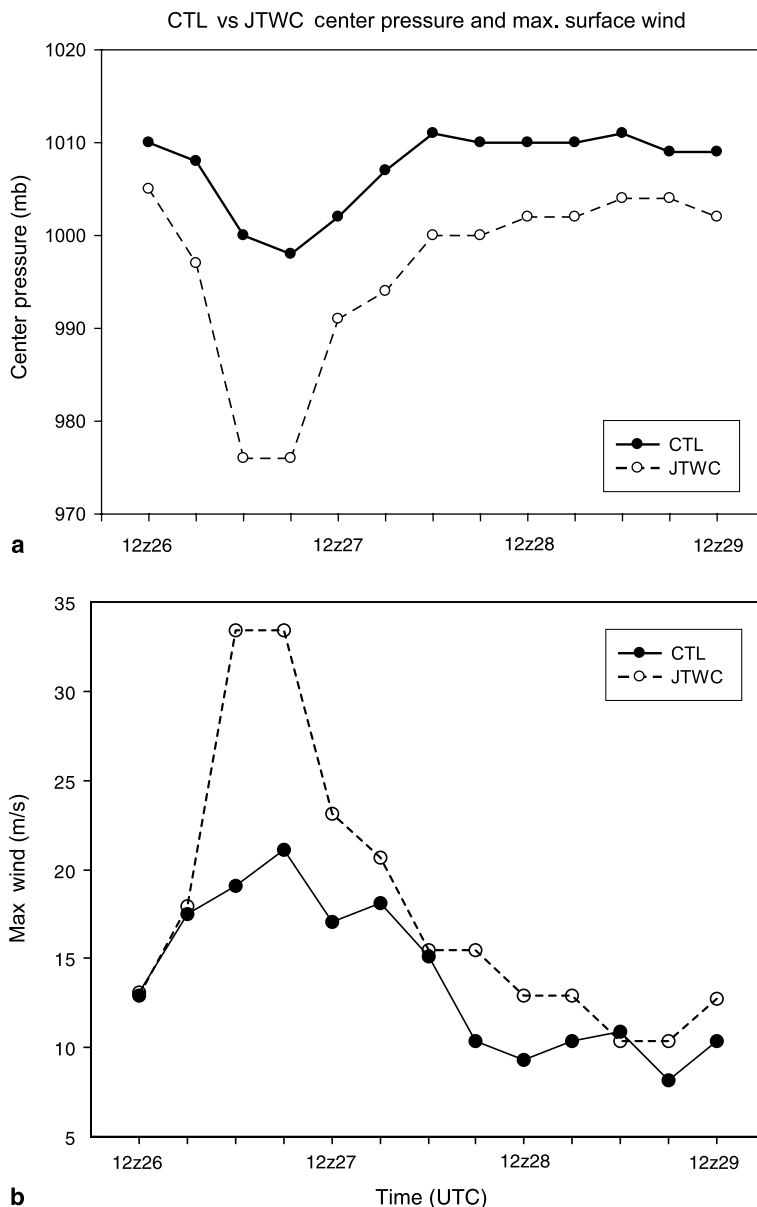


Fig. 12. The comparison of (a) central pressure, and (b) maximum surface wind speed between the model simulation (solid) and the JTWCs (dotted) best track database

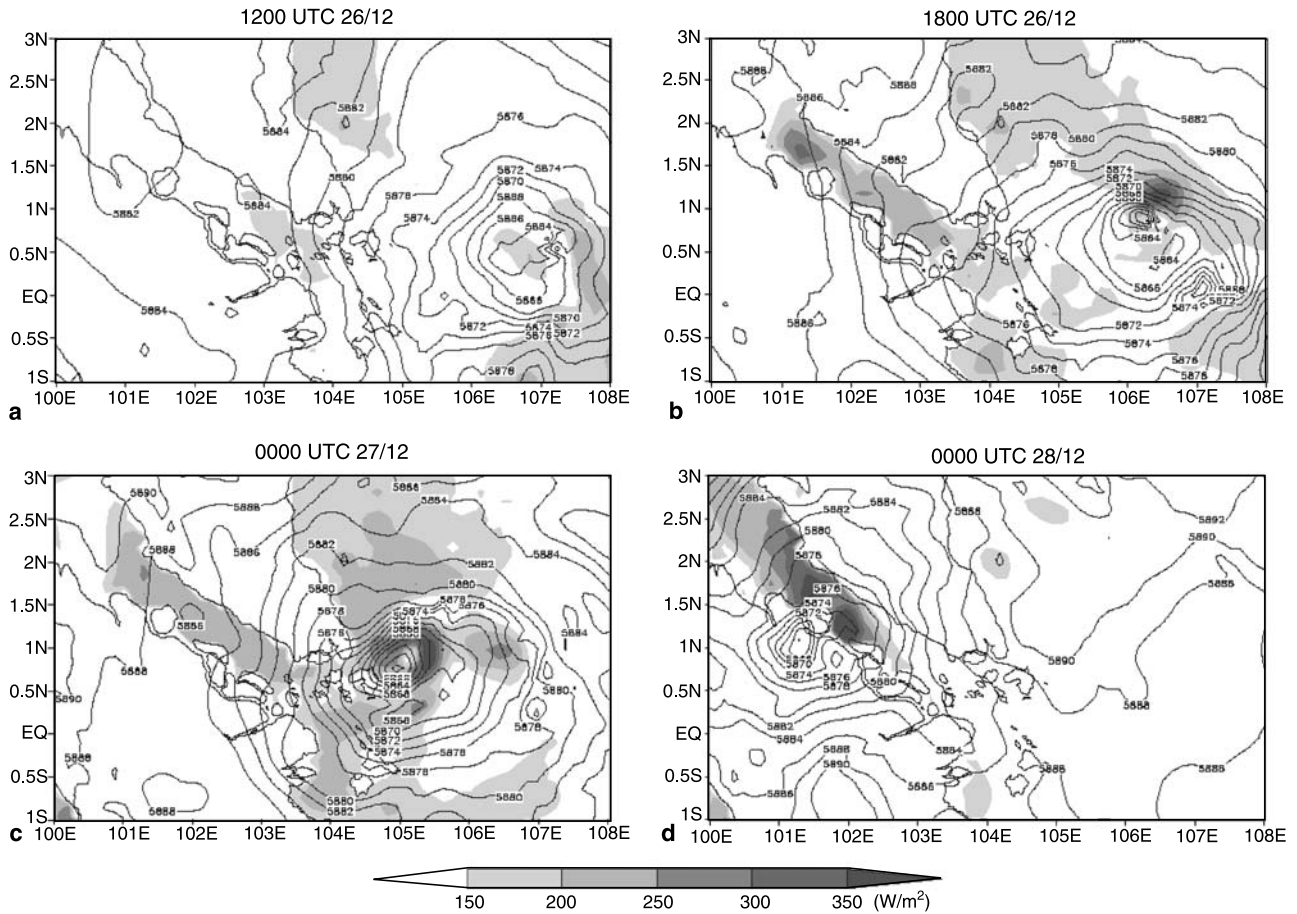


Fig. 13. The model 500 hPa geopotential height (contoured in m) and latent heat flux (shaded – W m^{-2}) valid at (a) 1200 UTC 26/12, (b) 1800 UTC 26/12, (c) 0000 UTC 27/12, and (d) 0000 UTC 28/12

JWTC values and the model output. Although the timing of the deepening of the central pressure was correctly simulated by the model, the magnitude was underestimated. The lowest simulated pressure was 998 hPa compared to less than 980 hPa of JWTC (Fig. 12a). Similarly, the maximum surface wind speed was also underestimated by the model (Fig. 12b) with the simulated speed of around 21 m s^{-1} compared to about 33 m s^{-1} of JWTC.

5.2 Diagnosis of simulation

Figure 13 shows the simulated 500 hPa height and oceanic latent heat flux at 1200 and 1800 UTC 26 December 2001, 0000 UTC 27 December 2001 and 000 UTC 28 December 2001. The sequence indicates the strengthening of the storm low-pressure centre and the intensification of the latent heat flux suggesting the role of air–sea interac-

tion in the development and evolution of the cyclone. At 1200 UTC 26 December 2001, an area of intense evaporation occurred east and south of the low pressure centre as indicated by the higher latent heat flux in the area (Fig. 13a). The 850 mb simulated wind plots indicate a strengthening of near surface wind ($> 10 \text{ m s}^{-1}$) in the area during the period suggesting the role of increased winds in extracting heat from the surface of the ocean (Fig. 14a). At 1800 UTC 26/12, the system strengthened rapidly with maximum latent heat fluxes ($> 350 \text{ W m}^{-2}$) just to the northeast of the storm centre with the 850 hPa wind speed exceeding 20 m s^{-1} (Fig. 14b). To the southeast of the vortex near 107° E , 0.5° N , there appeared to be another secondary low at the 500 hPa level which was associated with low level convergence at about 107° E as indicated in Fig. 14b. To the south of the main vortex, the wind speeds were comparatively weak with relatively low values of

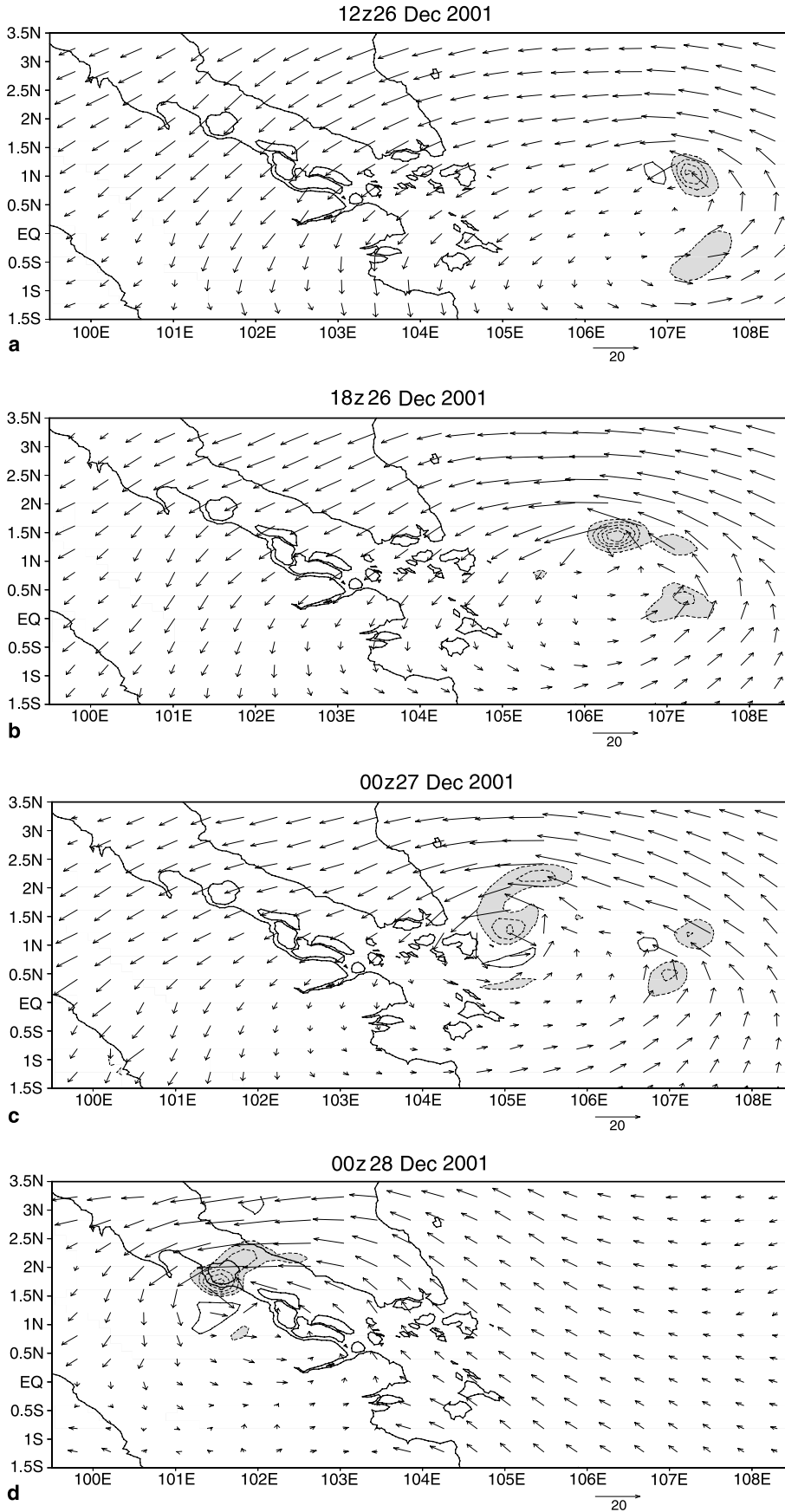


Fig. 14. The simulated 850 hPa horizontal wind vector (vector) and the 950 hPa wind field convergence (contour, convergence regions are shaded) valid at (a) 1200 UTC 26/12, (b) 1800 UTC 26/12, (c) 0000 UTC 27/12, and (d) 0000 UTC 28/12

surface latent heat flux (Fig. 13b). At 0000 UTC 27/12, several hours before the JWTC upgraded the system to a typhoon, the simulated system

strengthened further with higher latent heat flux near the centre of the vortex (Figs. 13c and 14c). It is noted that the region to the southeast of the

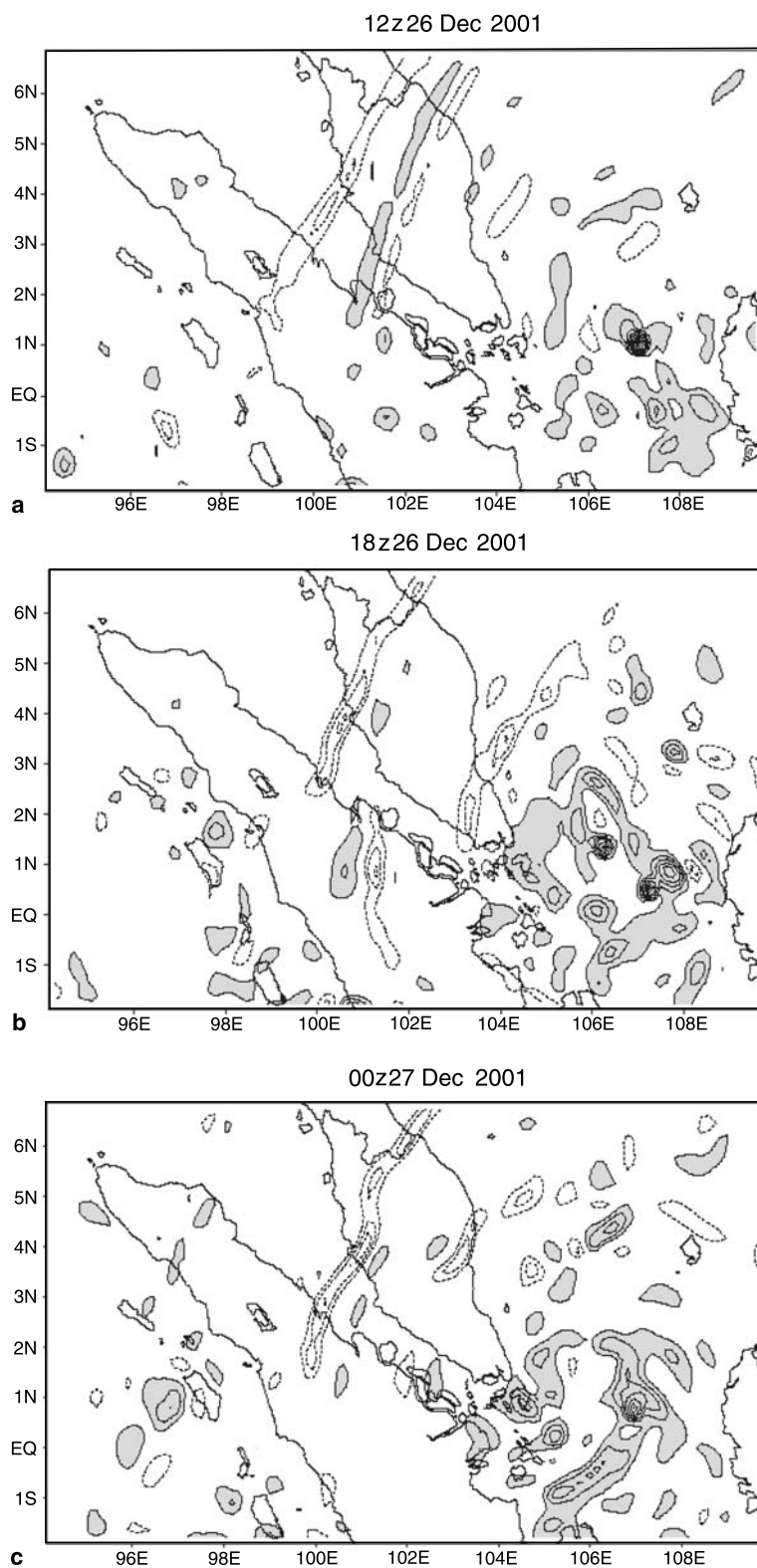


Fig. 15. As in Fig. 14, except for simulated 200 hPa divergence field (divergence regions are shaded)

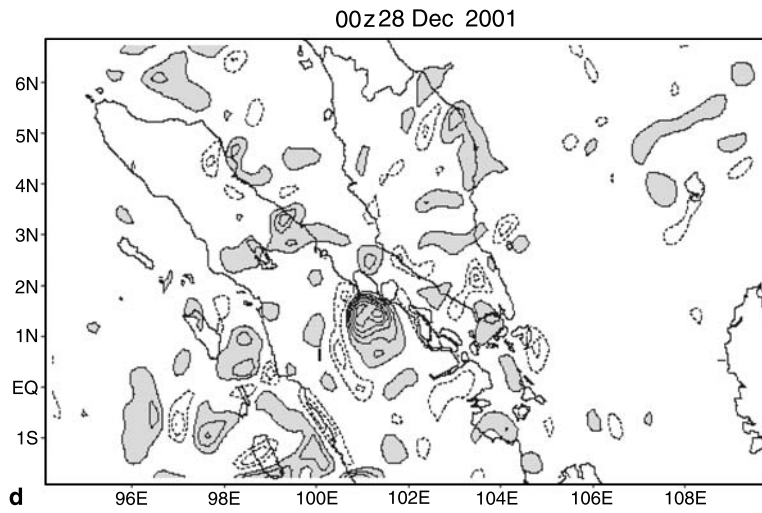


Fig. 15 (continued)

vortex centre continued to show relatively weak latent heat flux although east of the vortex centre, there was a secondary latent flux maximum. The

locations of these two latent heat maxima correspond well with the two regions of heavy rainfall in Fig. 4a. In between these two regions, the

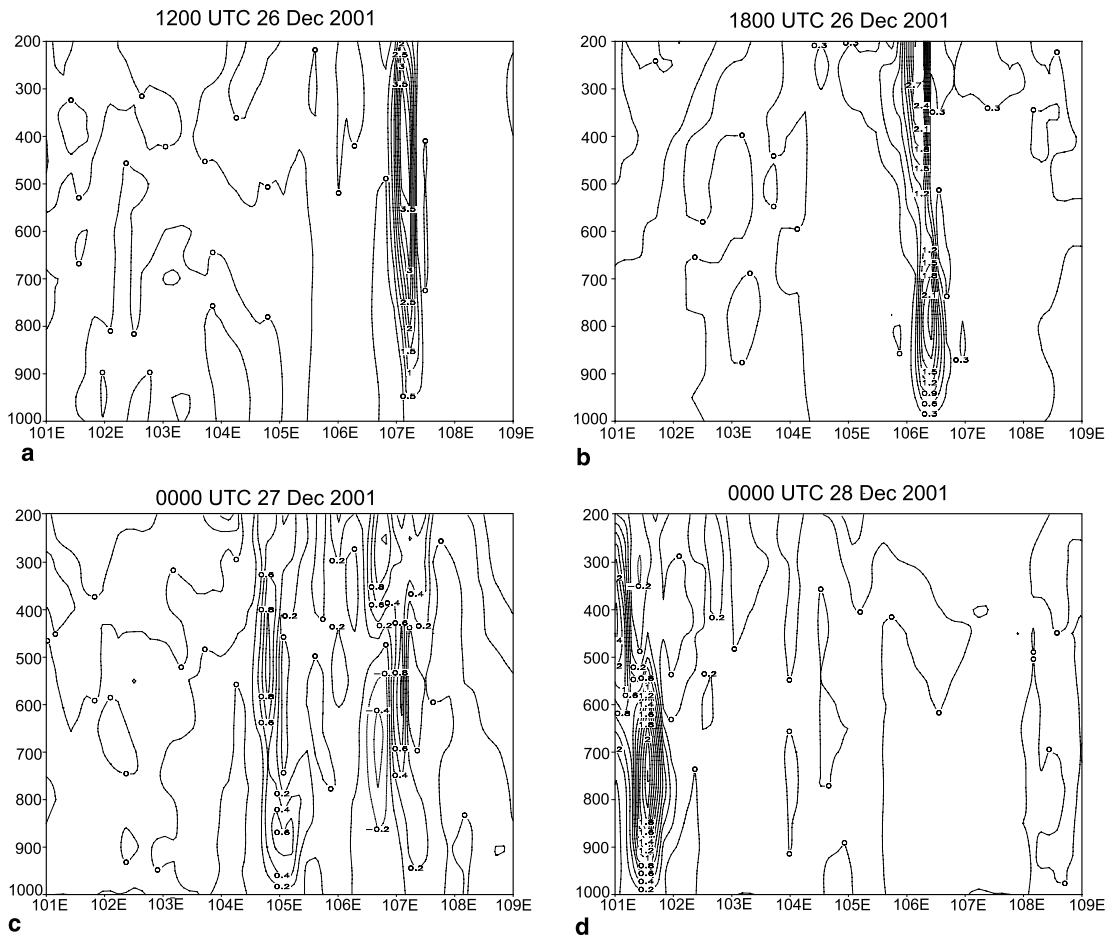


Fig. 16. East–west cross-section of the vertical velocity through the model storm at (a) 1200 UTC 26/12, (b) 1800 UTC 26/12, (c) 0000 UTC 27/12, and (d) 0000 UTC 28/12. Unit is $m s^{-1}$ and positive values indicate upward motion

latent heat fluxes are minimal. This area of weak evaporation roughly corresponds to that showing reduced rainfall in the simulated (Fig. 10a) and observed (Fig. 4a) fields.

The cyclone lost its strength once it made landfall at the southern tip of Malay Peninsula and, by 0000 UTC 28/12, it was located over Sumatra and the centre had weakened considerably (Fig. 13d). The surface westerlies south of the storm centre were much weaker although the easterlies north of the storm centre were still strong (Fig. 14d). These stronger easterlies were associated with higher latent heat fluxes from the Strait of Malacca (Fig. 13d). At 500 hPa, the circulation was similar to that at 850 hPa except with stronger wind due to less orographic influence (not shown).

At 200 hPa, positive divergence at the storm centre indicates that mass was being evacuated at the top of the storm in the model (Fig. 15). At 1200 UTC 26/12, a centre of positive divergence was located around 1° N, 107° E (Fig. 15a). The east–west cross section through the model storm shows positive values of vertical velocity from lower to upper levels indicating strong upward motion at 200 hPa in the centre (Fig. 16a). At 1800 UTC 26/12, as the storm further strengthened, the area of positive divergence expanded to cover approximately $104\text{--}108^{\circ}$ E, 1° S– 3° N (Fig. 15b) with an intensified but narrower region of ascent (Fig. 16b). At 0000 UTC 27/12, several hours before it made landfall at the southern tip of Malay Peninsula, two centres of divergence were established, one near the southern tip of the peninsula and the other at approximately 107° E (Fig. 15c). Two regions of upward motion were evident at that time with the upward motion at 200 hPa at the centre near the tip of the peninsula stronger than that at 107° E (Fig. 16c). The two ascent regions are likely to be associated with the aforementioned two low-level convergence circulations whereas the sinking motion is associated with the zone of less rainfall in the area between the two low-level convergence centres.

At 0000 UTC 28/12, an area of positive divergence at 200 hPa was located over Sumatra (Fig. 15d) indicating that mass was still being evacuated at the top of the storm. The cross-section through the storm indicates strong upward motion from lower to upper levels still being maintained and was likely associated with the

strong surface latent heat flux in the Strait of Malacca (Fig. 13d).

6. Conclusions

In this study, we used the non-hydrostatic version 3.6 of the MM5 model to simulate the near-equatorial tropical cyclone Vamei. Despite several discrepancies between the simulated and the observed values, overall the MM5 performed reasonably well in simulating this rare event. The simulated storm track compares well to the JWTC's best track. The simulated rainfall distribution also matches reasonably well compared to the observed TRMM rainrates. Validation with observed station data provides some confidence that the storm structure simulated by MM5 is realistic. Although not attempted here, it is possible that the model performance could be improved further by the introduction of vortex bogussing in the model first guess field (Kurihara et al, 1993; Zou and Qingnong, 2000) or an analysis-nudging technique (e.g., Mohanty et al, 2004).

Diagnosis of the simulated storm indicate the important of air–sea interaction and latent heat flux in the genesis and evolution of Vamei. As discussed in Chang et al (2003), the interaction between the Borneo vortex and a strong northeast monsoon cold surge contributed to the formation of Vamei. The storm subsequently moved westward partly due to the strong easterly steering wind blowing from Borneo. However, the strengthening of the storm to typhoon intensity several hours prior to landing, as reported by the JWTC, is interesting. The current simulation did not address this issue. However, a possible factor that could have contributed to the strengthening of the tropical cyclone Vamei is the warmer sea surface temperature (SST) off the eastern coast of Malay Peninsula. Examination of the TRMM weekly SST a week prior to formation of Vamei (not shown) indicated a very strong zonal SST gradient in the region. Further experimentation with MM5 is required to investigate this aspect.

Acknowledgements

We are grateful to MMD, CIRES-NOAA CDC, JTWC, TRMM for providing various datasets. This research is funded by the Malaysian Government IRPA grant no. 08-02-02-0012-EA215.

References

- Anthes RA (1982) Tropical cyclones: their evolution, structure and effects. Boston: Amer Meteor Soc, 208 pp
- Chang CP, Liu CH, Kuo HC (2003) Typhoon Vamei: an equatorial tropical cyclone formation. *Geo Res Lett* 30: 1150
- Chang CP, Harr PA, Chen HJ (2005) Synoptic disturbances over the equatorial South China Sea and western maritime continent during boreal winter. *Mon Wea Rev* 133: 489–503
- Emanuel KA (1986) An air-sea interaction theory for tropical cyclones. Part I: Steady-state maintenance. *J Atmos Sci* 43: 585–604
- Farfán LM, Zehnder JA (2001) An analysis of the landfall of hurricane Nora (1997). *Mon Wea Rev* 129: 2073–2088
- Fortner LE (1958) Typhoon Sarah, 1956. *Bull Amer Meteor Soc* 39: 633–639
- Holliday CR, Thomson AH (1986) An unusual near equatorial typhoon. *Mon Wea Rev* 114(12): 2674–2677
- Johnson RH, Houze RA Jr (1987) Precipitating clouds systems of the Asian monsoon. In: *Monsoon meteorology* (Chang C-P, Krishnamurti TN, eds). Oxford University Press, pp 298–353
- Kain JS, Fritsch JM (1993) Convective parameterization for mesoscale models: the Kain-Fritsch scheme. *Meteor Monogr* 46: 165–170
- Kurihara Y, Tuleya RE, Ross RJ (1993) An initialization scheme of hurricane models by vortex specification. *Mon Wea Rev* 121: 2030–2045
- Lim H, Chang CP (1981) A theory for mid-latitude forcing of tropical motions during winter monsoons. *J Atmos Sci* 38: 2377–239
- Liu Y, Zhang DL, Yau MK (1997) A multiscale numerical study of hurricane Andrew (1992). Part I: Explicit simulation and verification. *Mon Wea Rev* 125: 3073–3093
- Mohanty UC, Mandal M, Raman S (2004) Simulation of Orissa Super Cyclone (1999) using PSU/NCAR Mesoscale model. *Natural Hazards* 31(2): 373–390
- Power JG, Davis CA (2002) A cloud-resolving, regional simulation of tropical cyclone formation. *Atmos Sci Lett* 3: 15–24
- Reynolds RW, Smith TM (1994) Improved global sea surface temperature analysis using optimum interpolation. *J Climate* 7: 929–948
- Rotunno R, Emanuel KA (1987) An air-sea interaction theory for tropical cyclones. Part II: Evolutionary study using axisymmetric nonhydrostatic numerical model. *J Atmos Sci* 44: 542–561
- Schultz P (1995) An explicit cloud physics parameterization for operational numerical weather prediction. *Mon Wea Rev* 123: 3331–3343
- Zhang DL, Anthes RA (1982) A high-resolution model of the planetary boundary layer – sensitivity tests and comparisons with SESAME-79 data. *J Appl Meteor* 21: 1594–1609
- Zhang DL, Chang HR, Seaman NL, Warner TT, Fritsch JM (1986) A two-way interactive nesting procedure with variable terrain resolution. *Mon Wea Rev* 114: 1330–1339
- Zou X, Qingnong X (2000) Studies on the initialization and simulation of a mature hurricane using a variational bogus data assimilation scheme. *J Atmos Sci* 57: 836–860

Corresponding author's address: Fredolin T. Tangang, School of Environmental and Natural Resource Sciences, Faculty of Science and Technology, National University of Malaysia, 43600 Bangi, Selangor, Malaysia (E-mail: tangang@pkrisc.cc.ukm.my)